Cell-free Expression and Rapid Analysis of Single-Chain Antibody Fragments

Katherine Dam and Jackson A. Buss, Ph.D.

INTRODUCTION

Single-chain antigen-binding fragments (e.g., VHH, scFv) are gaining popularity in the therapeutic field, as they offer several advantages over traditional antibodies, including smaller size, increased permeability, and enhanced solubility and thermal stability (Figure 1–2). Here, we demonstrate the utility of our cell-free protein synthesis (CFPS) platform, NEBExpress® Cell-free *E. coli* Protein Synthesis System (NEB #E5360), for the rapid production of antibody fragments in quantities suitable for purification or direct analysis via Biolayer Interferometry (BLI) (Figure 3–6). CFPS workflows are fast, scalable, and cost-efficient, and can be seamlessly integrated with high-throughput DNA assembly methods to rapidly screen diverse binder libraries. Additionally, the defined nature of these CFPS systems allows for straightforward optimization to improve expression of challenging constructs. The approaches described herein offer a fast and efficient screening method for the discovery and initial characterization of novel antibody fragments.

MATERIALS AND METHODS

Cell-free production and purification of VHH and scFv

Genes for anti-GFP VHH-1, anti-GFP VHH-2, anti-HER2 scFv-1, and anti-HER2 scFv-2 were codon-optimized for expression in *E. coli* and assembled into a pET28 vector under the T7 promoter with C-terminal 6xHis-tags. Sequence-validated plasmids were purified with Monarch® Spin Plasmid Miniprep Kit (NEB #T1110), diluted to 50 ng/µl and used as templates for 100 µl NEBExpress Cell-free *E. coli* Protein Synthesis (CFPS) (NEB #E5360) reactions (Table 1C). Optimal expression was achieved at 37°C and performed in 2 ml 96-deepwell plates (Thermo 95040460Bf) for 5 hours with 500 rpm shaking. The His-tagged proteins were purified with NEBExpress Ni-NTA Magnetic Beads (NEB #S1423) on an automated particle processor (e.g., KingFisher® Apex), as described previously (1). Briefly, 100 µl Ni-NTA beads were resuspended in 200 µl 2X Lysis/Binding Buffer (40 mM sodium phosphate, 600 mM NaCl, 20 mM Imidazole, pH 7.4), diluted with 100 µl nuclease-free water and applied to each 100 µl CFPS reaction for 30 min. Beads were then transferred to 400 µl/well Wash Buffer (20 mM sodium phosphate, 300 mM NaCl, 20 mM Imidazole, pH 7.4) for 5 min. This wash step was repeated and the purified proteins eluted in 50 µl/well Elution Buffer (20 mM sodium phosphate, 300 mM NaCl, 250 mM Imidazole, pH 7.4) for 10 min. All steps employed slow agitation. Biological replicates (n) of the expressed and purified samples for each fragment were visualized via SDS-PAGE electrophoresis (Table 2; Figure 4A and 6A) and analyzed for yield and purity (Table 2) by capillary electrophoresis on a Revvity LabChip® GXII Touch™ using the Protein Express Assay Reagent Kit (#CLS960008).

MATERIALS

- NEBExpress® Cell-free *E. coli* Protein Synthesis System (NEB #E5360)
- Monarch® Spin Plasmid Miniprep Kit (NEB #T1110)
- NEBExpress Ni-NTA Magnetic Beads (NEB #S1423)
- NEBuilder® HiFi DNA Assembly Master Mix (NEB #E2621)
- NEB® 10-beta Competent *E. coli* (High Efficiency) (NEB #C3019)
- SHuffle® T7 Competent *E. coli* (NEB #C3026)
- phi29-XT RCA Kit (NEB #E1603)

FIGURE 1: **DNA to Data in One Day**

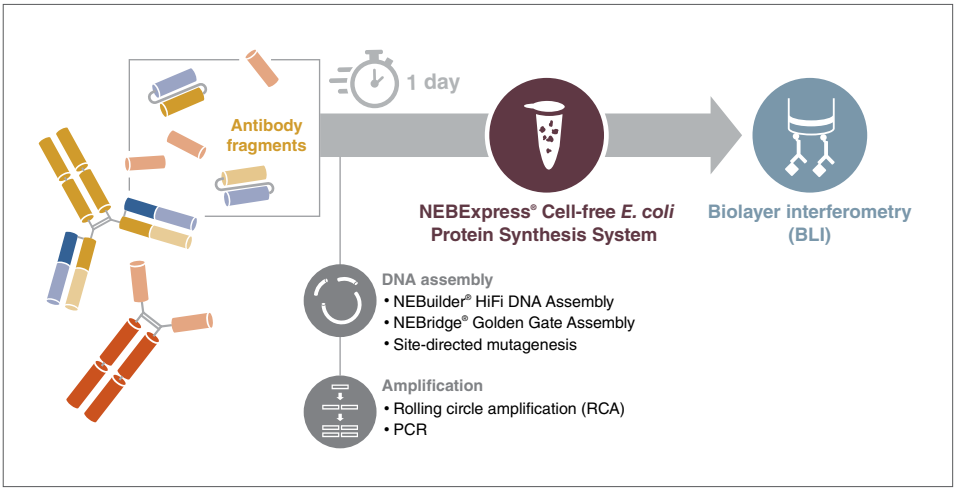

Single-chain antibody fragments can be rapidly produced with the NEBExpress CFPS system and directly analyzed for binding via BLI. Templates for CFPS must include a T7 Promoter but can take the form of purified plasmid or a variety of amplified products, including PCR or RCA products, thus supporting a variety of upstream assembly or mutagenesis strategies.

TABLE 1A: **NEBuilder HiFi DNA Assembly**

NEBUILDER HIFI DNA ASSEMBLY REACTION COMPONENTS	STANDARD RXN (µl)	MINIATURE RXN (µl)	MASTER MIX 20X (µl)
Vector*	varied	0.5	10
Insert	varied	1	–
2X NEBuilder DNA Assembly Master Mix	10	2.5	50
Nuclease-free Water	up to 20	1	20
Total Volume (µl):	**20**	**5**	**80**

*PCR ampliifed, purified and DpnI-treated (NEB #R0176)

TABLE 1B: **phi29-XT RCA**

PHI29-XT RCA REACTION COMPONENTS	STANDARD RXN (µl)	MINIATURE RXN (µl)	MASTER MIX 40X (µl)
Resuspended Colony	varied	1	–
phi29-XT Reaction Buffer (5X)	4	1	40
dNTPS Solution Mix (10 mM)	1	0.5	20
Exo-Resistant Primers (500 µm)	1	0.5	20
Nuclease-free Water	up to 18	1.5	60
phi29-XT DNA Polymerase	2	0.5	–
Total Volume (µl):	**20**	**5**	**140**

TABLE 1C: **NEBExpress *E. coli* Cell-Free Protein Synthesis**

NEBEXPRESS CELL-FREE *E. COLI* PROTEIN SYNTHESIS REACTION COMPONENTS	STANDARD 2X RXN		MASTER MIX 40X (µl)
	PLASMID TEMPLATED (µl)	RCA TEMPLATED (µl)	
Template	10	2.5	–
Synthesis Buffer	50	25	1000
S30	24	12	480
RNAse Inhibitor	2	1	40
T7 RNAP	2	1	40
GamS	–	1	–
Nuclease-free Water	6	7.5	300
Total Volume (µl):	**94**	**50**	**1860**

TABLE 2: **Purified CFPS products**

SAMPLE	SIZE (kDa)	CONC (ng/µl)	PURITY	N
VHH-1	13.7	57.2 ± 1.9	99.7 ± 0.2	3
VHH-2	14.6	60.5 ± 1.4	99.6 ± 0.4	3
scFv-1	27.6	24.5 ± 1.4	87.0 ± 4.5	3
scFv-2	28.7	73.6 ± 7.6	99.3 ± 0.1	3

NEBuilder HiFi mutagenesis and cell-free/cell-based expression

DNA fragments containing the desired VHH-1 mutations (Table 3) were synthesized and directly assembled into a complementary pET28 vector via NEBuilder HiFi DNA Assembly Master Mix (NEB #E2621) (Table 1A). Inserts were designed to provide 19–21 bp overlaps with the vector, each exhibiting a Tm of ~64°C. Assembly reactions were introduced via transformation into NEB® 10-beta Competent *E. coli* (High Efficiency) (NEB #C3019) and selected on LB agar plates supplemented with Kanamycin 50 µg/ml (LB-Kan) at 30°C overnight. Constructed plasmids were purified with Monarch Spin Plasmid Miniprep and the mutations were validated via next-generation sequencing. Confirmed plasmids were introduced into SHuffle® T7 Competent *E. coli* (NEB #C3026) (2,3) by transformation and selected on LB-Kan at 30°C. Fresh transformants were applied directly to the phi29-XT RCA Kit (NEB #E1603) reaction mix according to standard protocols (Table 1B). After 2 hours at 42°C, the amplified plasmid DNA for each construct was used to template coupled transcription-translation in a standard 50 µl NEBExpress CFPS reaction (Table 1C) at 37°C for 5 hours with 500 rpm shaking.

BLI crude sample preparation and analysis

We used the Octet® RH16 (Sartorius®; Figure 3) to characterize the binding of VHH-1 mutants to their antigen, enhanced GFP (eGFP) (4). Prior to use, Octet NTA biosensors (Sartorius #18-5101) were rehydrated in 200 µl/probe BLI Buffer 1 (20 mM sodium phosphate, 150 mM NaCl, 0.1% Tween-20, 0.05 mg/ml BSA, pH 7.4) for 10 min. BLI Buffer 1 proved crucial to our success and was used for all washes and dilutions. CFPS reactions expressing His-tagged VHH-1 mutants were diluted 1:4-16 and applied directly as a crude ligand (i.e., Load) to the equilibrated Ni-NTA probes. The association phase was measured with eGFP at 180 nM. For analysis of anti-HER2 scFvs, similar dilutions of crude ligand were analyzed against 100 nM recombinant Human Her2/ERBB2 Protein (ECD) (Sino Biological® #10004-HCCH). Dilutions were made using BLI Buffer 2 (1X PBS, 0.25% Tween-20, 0.5 mg/ml BSA, pH 7.4). For all samples and washes, 50 µl/well was transferred to Octet 384TW plates for analysis at 30°C with 1200 rpm shaking using the following protocol: Baseline1, 60 s; Load, 300 s; Baseline2, 600 s; Baseline3, 600 s; Association = 600 s; Dissociation, 600 s. Analysis of the BLI kinetic measurements was performed on the Octet Analysis Studio using a partial 1:1 binding model.

FIGURE 2: **Antibodies and Antibody Fragments.**

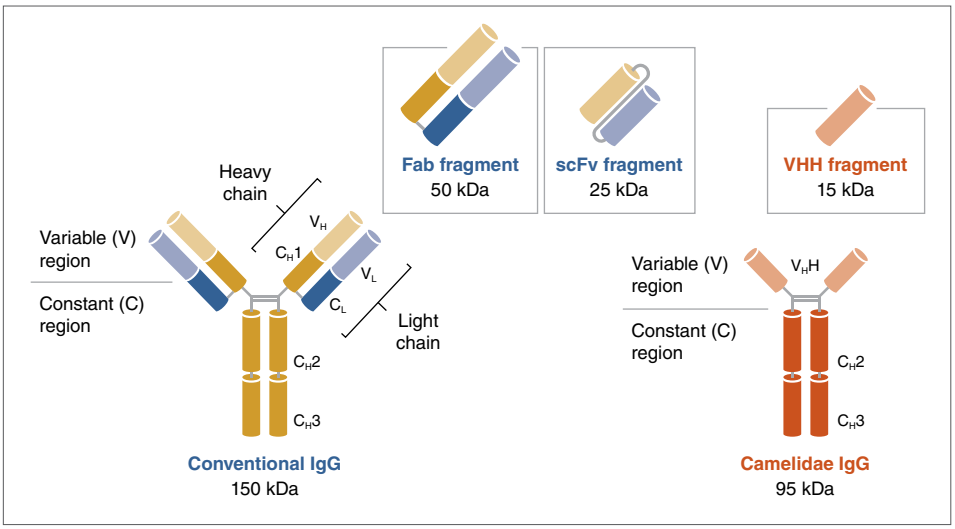

Conventional IgGs consist of two heavy chains and two light chains, linked together with essential disulfide bonds. The Fab fragment comprises the variable and adjacent constant regions of both chains and is sufficient for antigen binding. Direct linkage of the Fab variable regions from both the light and heavy chains creates an scFv fragment, or single-chain variable fragment, with the linker length, composition and relative arrangement significantly impacting binding and solubility. Camelidae IgGs are smaller than conventional IgGs, consisting of two heavy chains, each presenting a single variable region for antigen binding. The heavy-chain only variable region from Camelidae is known as a VHH fragment.

Validation of BLI data with purified ligands

Representative VHH-1 mutants (S35A, R59A, N99A, N101A, E105A) and a wild-type control that sampled the observed range of binding affinities were purified (Figure 5A), analyzed via BLI and compared to the CFPS data (Figure 5B). SHuffle T7 Competent *E coli* cells (2,3) containing sequence-validated plasmids were grown in 50 ml LB, induced with 1 mM IPTG at 30°C with 250 rpm shaking, and processed for purification with NEBExpress Ni Spin Columns (NEB #S1427) according to standard protocols. Eluted proteins were dialyzed in Storage Buffer (20 mM sodium phosphate, 150 mM NaCl, 50% (v/v) glycerol) and confirmed for yield and purity via SDS-PAGE (Figure 5A). The six ligands were analyzed at 500 nM against a range of eGFP concentrations (1.6-100 nM) using the Octet NTA probes and a similar kinetics acquisition program defined above, with the association and dissociation acquisitions reduced to 300s (Figure 5B). Prior to fitting the grouped data with a full 1:1 binding model, a Savitzky-Golay filter was applied, and a double reference subtraction was performed. The fitted binding constants for the purified proteins were plotted against those from the screening data to visualize their linear relationship (Figure 5B, inset).

RESULTS

Rapid cell-free production and purification of VHH and scFv

Coupling cell-free expression to affinity purification with Ni-NTA magnetic beads enables a streamlined and automatable approach to rapidly generate analytical amounts of diverse target proteins in hours instead of days (Figure 1).

When visualized by Coomassie-stained SDS-PAGE gels, bands corresponding to the appropriate sizes for VHH-1 and VHH-2 (Table 2) were apparent above the lysate background (Figure 4A). Purified samples of VHH-1 and VHH-2 were all ~60 ng/µl, exhibiting high purity (>95%) and low variance between replicates (< 10% CV). These results demonstrate that the NEBExpress CFPS system reproducibly produces analytical amounts of soluble VHHs without additional supplementation. To assess whether the soluble VHHs produced by NEBExpress CFPS were properly folded and retained binding activity, we performed BLI-based binding assays with the Octet RH16.

Direct BLI analysis of VHHs from NEBExpress CFPS

We selected 15 residues of anti-GFP VHH-1 that would potentially disrupt its interaction with eGFP (4) and constructed single-point mutants using NEBuilder HiFi DNA Assembly. Two transformants of each mutant, along with a wild-type (wt) control, were plasmid-purified and sequence-verified. At least one clone of each construct was determined to be 100% correct. For the 32 clones sequenced, 27 were validated, indicating a cloning efficiency of ~85%.

Each validated construct was expressed in the NEBExpress CFPS system and the crude CFPS reaction was used directly as the ligand for BLI kinetic measurements. The Octet NTA probes specifically capture the anti-GFP-VHHs and

TABLE 3: **Kinetic Analysis of Unpurifed VHHs**

SAMPLE	MUTATION	EFFECT	CFPS K_D (nM)	PURIFIED K_D (nM)
	C24A	disulfide	19	—
	S35A	contacts GFP	7	6
	R37A	contacts GFP	9	—
	Y39A	contacts GFP	16	—
	A42A	control, wt	6	—
	E46A	contacts GFP	13	—
	W49A	contacts GFP	8	—
	R59A	contacts GFP	338*	220
	V66P	unknown	4	—
	C98A	disulfide	8	—
	N99A	unknown	125*	52*
	N101A	contacts GFP	227*	123
	G103A	contacts GFP	7	—
	F104A	contacts GFP	8	—
	E105A	contacts GFP	29	15
	wt	plasmid control	9	6

FIGURE 3: **Biolayer Interferometry (BLI) measures the change in mass at the surface of a biosensor by detecting shifts in the interference pattern of reflected white light**

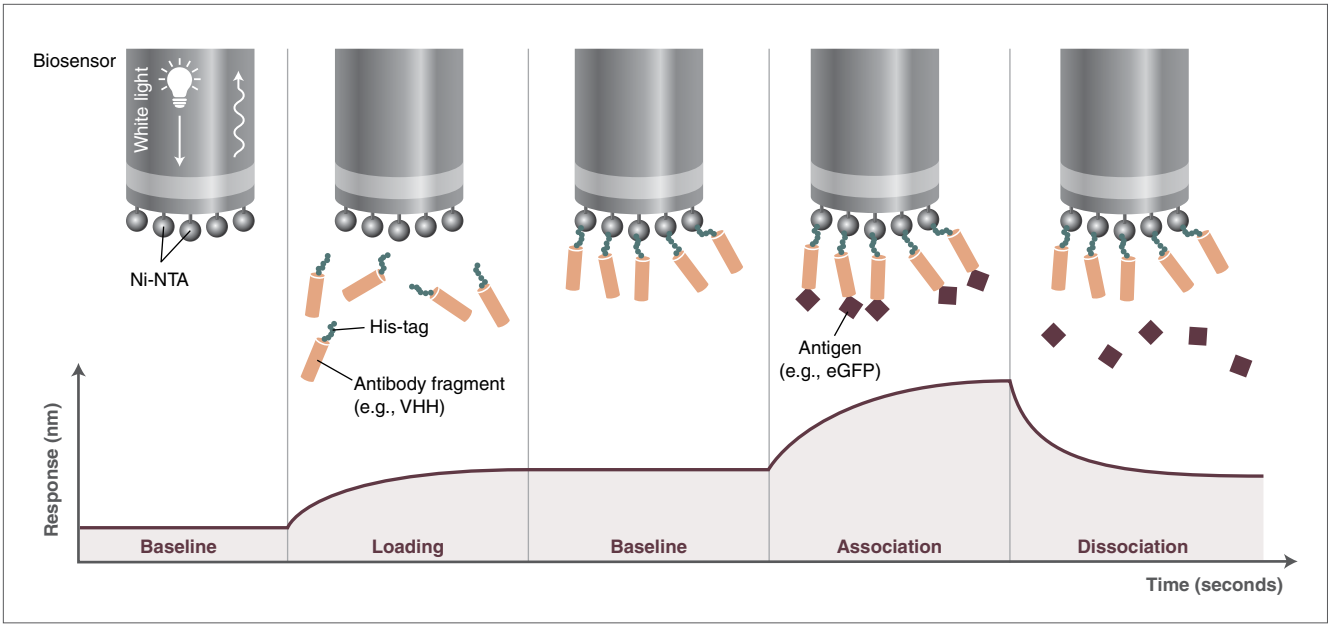

Following a baseline in diluent, the coordinated Ni^{+2} of the NTA probes associates with the target ligand (e.g., VHH) via its hexahistidine tag (i.e., load), the loaded ligand is then transferred to diluent to remove impurities and generate a new baseline, the washed ligand is dipped into purified antigen (e.g., eGFP) to measure the observed rate of association (k_{obs}) and then dipped back into diluent to measure the rate of dissociation (k_d). From these rates and the known antigen concentration, the rate of association (k_a) and the binding constant (K_D) can be calculated.

subsequently monitor their interaction with their purified antigen, eGFP (Figure 4B, Table 3). For 13 of 16 VHH-1 constructs, the ligands produced via CFPS generated high-quality kinetic binding data that was well fit with a partial 1:1 model (average R^2Assoc = 0.99). These results demonstrate the potential to obtain high-quality BLI data directly from CFPS inputs.

The three constructs whose data were fit poorly (R59A, N99A, and N101A) displayed the worst binding affinity to eGFP, suggesting that the disruption of the eGFP interaction and not the quality of the ligand, amplified the fitting error. Mutations exhibiting significant effects, regardless of fitting, along with mutations (e.g., E105A) exhibiting more moderate effects were identified as hits for further characterization.

Validation of crude BLI analysis with purified VHH-1 mutants

The three constructs of anti-GFP VHH-1 (R59A, N99A, N101A) that exhibited the most significant effect on eGFP binding were purified along with a wild-type control and two additional constructs (E105A, S35A) that showed moderate to no effect on binding. These purified samples (Figure 5A) were analyzed with BLI using standard approaches and the fitted data were compared to that of the crude CFPS ligands (Figure 5B, Table 3). The kinetic analyses of these anti-GFP VHH-1 constructs were well fit by a full 1:1 model with an average R^2 Full > 0.98, and the resulting K_D's showed good agreement with the crude CFPS samples (R^2 = 0.98; Table 3). The conserved trend observed in eGFP binding for the purified ligand and crude CFPS ligand (Figure 5B) validates the rapid cell-free BLI workflow described herein.

Kinetic binding analysis of crude anti-Her2 scFvs from CFPS

The Cell-free expression and automated affinity purification of antibody fragments are not limited to VHHs and can be readily applied to scFvs without the need for supplementation. When visualized by Coomassie-stained SDS-PAGE gels, bands corresponding to the appropriate sizes for scFv-1 and scFv-2 (Table 2) were apparent above the lysate background for all replicates (Figure 6A). Purified proteins migrated similarly with measured concentrations of 25 or 80 ng/µl for scFv-1 and scFv-2, respectively. The purified scFvs all displayed a similar high purity (>95%) and low variance between replicates (<10% CV) as the VHHs. The same procedure outlined above for kinetic analysis of crude VHH-1 mutants produced from CFPS was applied to anti-HER2 scFv-1 and scFv-2 to confirm proper folding and activity (5). The BLI kinetic analysis of scFvs produced directly from CFPS were fit well (R^2 Full > 0.95) and produced K_D's for anti-HER2 scFv-1 (K_D = 4.3 nM) and scFv-2 (K_D = 4.9 nM) that showed good agreement with published values (K_D = 4.8 nM and 5.3 nM, respectively). These results illustrate the robust application of this screening method to more complex single-chain antibody fragments. Note that while the apparent expression and overall yield of scFv-2 were significantly higher than that of scFv-1, the measured K_D's show that scFv-1 binds similarly, if not tighter. This result questions the need for optimizing expression at the screening stage.

DISCUSSION

Cell-free expression of antibodies

For the VHHs and scFvs characterized in this study, sufficient yields from standard NEBExpress CFPS reactions were achieved to support downstream analysis via BLI. Furthermore, BLI analysis of these antibody fragments was possible directly from CFPS reactions without any purification, thereby streamlining this workflow. It is important to note that while cell-free expression observed for these targets was lower than that typically observed for cell-free reference standards (e.g., GFP, DHFR, etc.), no supplementation was provided to enhance expression. The production of antibodies in bacterial systems is notoriously

nebulous, and optimal expression conditions need to be validated empirically. Many have shown that supplementary elements or chemical additives can be used to enhance the overall yield of antibody production, including solubility and affinity tags (e.g., MBP, SUMO, GST), disulfide affecting agents (GSH:GSSG, DTT, TCEP) or elements (e.g., DsbC, PDI), chaperones (e.g., GroEL/ES, DnaJK, FkpA, Skp), protease inhibitors (e.g., Leupeptin, Pepstatin A) and solubilizing agents (e.g., arginine, etc.). Additionally, soluble yield can often be improved with longer incubation (>12 hours) at lower temperatures (16–25°C). For proteins where soluble expression remains challenging, solubilization of unfolded or misfolded material followed by refolding remains a viable strategy, as previously described (6). Such approaches are readily adaptable to both cell-based and cell-free workflows and can be implemented at scale when necessary.

Importantly, the open and modular nature of CFPS enables rapid and systematic exploration of these parameters without the constraints imposed by cellular viability. This flexibility is particularly advantageous for antibody fragments, where folding efficiency and disulfide bond formation are primary determinants of functional yield. While antibodies produced in *E. coli* –based CFPS systems lack glycosylation, this feature can be advantageous for certain applications, including antibody-drug conjugates and site-specific labeling strategies. Moreover, CFPS readily supports the incorporation of non-canonical amino acids, enabling precise chemical conjugation and functional diversification that is difficult to achieve *in vivo*.

Finally, while this study focused on antibody fragments, it is worth noting that full-length IgG production in engineered *E. coli* strains (e.g., SHuffle) has been extensively demonstrated, highlighting the continued convergence of bacterial and cell-free platforms for increasingly complex antibody architectures (1,2). Together, these observations position CFPS as a powerful and complementary platform for rapid antibody prototyping, optimization, and functional characterization.

Tips for BLI data acquisition

The loading range for crude and purified ligands in both BLI and Surface Plasmon Resonance (SPR) methods depends on the expression of the sample and the chosen probe or sensor type. For this analysis, we generated high-quality data with the Octet NTA probes using a broad range of crude ligand dilutions, ranging from 2- to 50-fold in BLI Buffer, though the optimal dilutions need to be empirically determined for each ligand-analyte combination. The most critical and time consuming step was optimizing the BLI buffer to block non-specific interactions between the complex load matrix (e.g., lysate) and the probe, while still enabling the specific interaction of the ligand with the analyte. Other probes, like the Octet Anti-Penta-His (HIS1K) Biosensors (Sartorius 18-5120) or Octet VHH Biosensor (Sartorius 18-5178), which rely on more specific probe-ligand interactions, may alleviate some of these difficulties.

FIGURE 4: **Expression and Analysis of VHHs directly from CFPS**

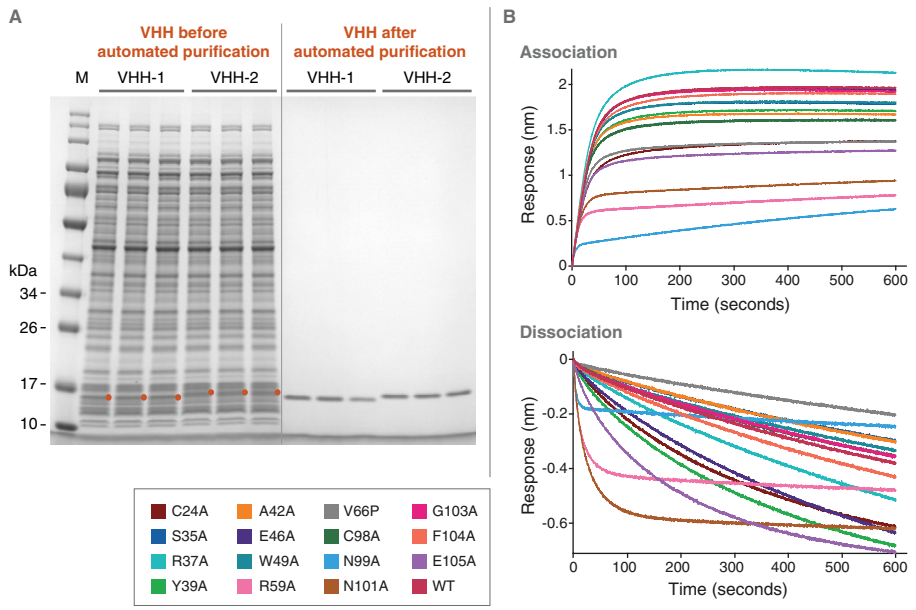

A) Coomassie-stained SDS-PAGE of anti-GFP VHH-1 and VHH-2 replicates expressed via NEBExpress CFPS shown before and after automated purification with Ni-NTA magnetic beads. Yield and purity are displayed in Table 2. (B) Representative BLI kinetic traces for the association (top) and dissociation (bottom) phase of sixteen VHH-1 variants (e.g., C24A, etc) expressed via NEBExpress CFPS and analyzed directly (before purification) via BLI with Octet NTA probes. The fitted data is shown in Table 3.

FIGURE 5: **BLI kinetic analysis of purified VHH-1 mutants**

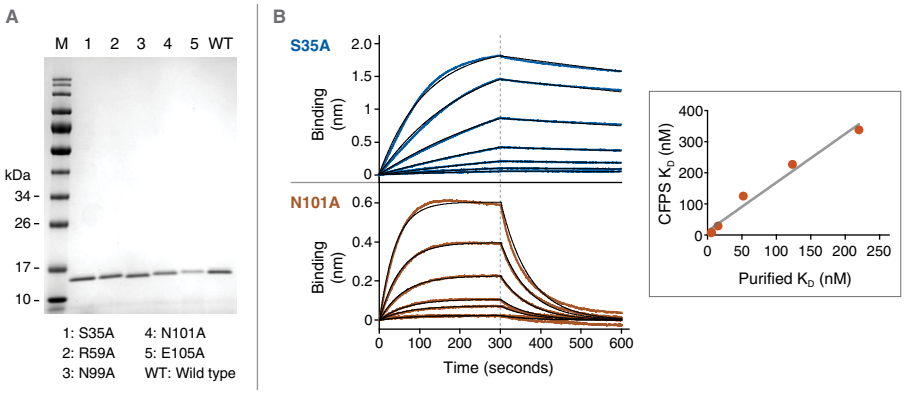

(A) Coomassie-stained SDS-PAGE of purified anti-GFP VHH-1 mutants – S35A, R59A, N99A, N101A, E105A, and wt. (B) Representative BLI kinetic traces (blue, maroon) and fitted curves (black) for the association (time 0-300 s) and dissociation (time= 300-600 s) phases of VHH-1 mutant S35A (blue) and N101A (maroon) binding to a range of eGFP concentrations (1.56-50 nM). Calculated K_Ds for purified ligands are plotted against calculated K_D's from NEBExpress CFPS system (inset), and fit with a linear regression, illustrating a strong correlation between the data generated from the two ligand sources: $R^2 = 0.98$.

FIGURE 6: **Expression, Purification and BLI analysis of scFv from CFPS**

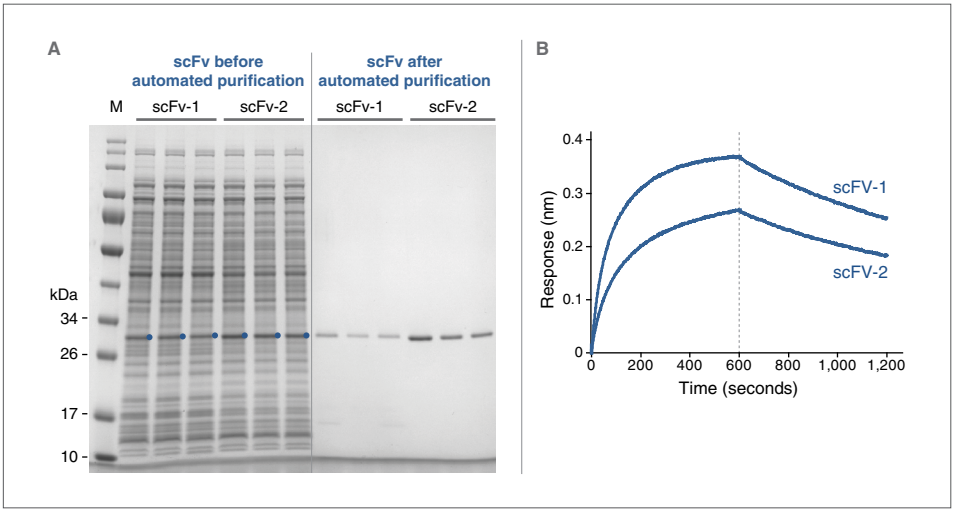

(A) Coomassie-stained SDS-PAGE of anti-HER2 scFv-1 and scFv-2 replicates expressed via NEBExpress CFPS shown before and after automated purification with Ni-NTA magnetic beads. Yield and purity are displayed in Table 2. (B) Representative BLI kinetic traces for the association (time 0–600 s) and dissociation (time= 600–1200 s) phases of crude anti-HER2 scFv-1 (blue) and scFv-2 (grey) against 100 nM HER2.

Additional Points/Comments

One of the benefits of CFPS is that transformation is not required. While the RCA described herein was templated by cellular transformants, these amplification reactions could have been templated by the NEBuilder HiFi reaction, as shown previously (7), thus further streamlining the process and increasing the accessible throughput.

The mutagenesis of VHH was performed using NEBuilder HiFi DNA Assembly of dsDNA fragments, – however, similar approaches using our NEBridge® Golden Gate Assembly Kits (NEB #E1601 or #E1602) or Q5® Site-Directed Mutagenesis Kit (NEB #E0554) can also serve as template for phi29-based RCA and NEBExpress CFPS.

References

1. Buss J, et al. (2024). NEB App Note.
2. Lobstein J, et al. (2012). Microb Cell Fact. 11(56).
3. Eaglesham JB, et al. (2021). Methods Enzymol. 659,105–144.
4. Kubala MH, et al. (2010). Protein Sci. 19(12), 2389–401.
5. Yun H, et al. (2024). Biotechnol J. 19(7), e2300745.
6. Rudolph R, Lilie H. (1996). FASEB J. 10(1), 49–56.
7. Lund S, et al. (2025). NEB App Note.